*Korean J. Chem. Eng.*, 36(9), 1410-1416 (2019)
DOI: 10.1007/s11814-019-0329-4

pISSN: 0256-1115
eISSN: 1975-7220

# Synthesis of mesoporous silica SBA-15 using a dropwise flow reactor

**Seong Chul Ryu, Jong Hwan Lee, and Hee Moon†**

School of Chemical Engineering, Chonnam National University, 77 Yongbong-ro, Gwangju 61186, Korea
(*Received 23 March 2019 • accepted 19 June 2019*)

**Abstract**−Generally, mesoporous silica materials, such as SBA-15, are hydrothermally synthesized in batch reactors. We synthesized SBA-15 in a dropwise flow reactor, which has several merits, such as short reaction times, continuous operation, and easy scale-up. The reaction system had three parts: a mixer and two reaction channels, one operated at a low temperature of 35 °C for the self-assembly of 2D hexagonal silica structures, and the other operated at a high temperature of over 80 °C to increase the stability of the silica structure. Two different operating schemes were used to mix the two immiscible reactant streams, one with a magnetically driven active mixer and the other with a direct supply of premixed reactants. The dropwise flow reactor with the active mixer instead of the low-temperature reaction channel produced fractured silica particles in the final product. However, when a premixed solution under hydrolysis conditions was employed, the synthesis of mesoporous silica SBA-15 was successful within 2.5 h in the dropwise flow reactor, showing close physical properties to the reference SBA-15 sample obtained in a conventional batch reactor.

Keywords: Flow Synthesis, Mesoporous Silica Materials, SBA-15, Dropwise Flow Reactor, Effect of Mixing

## INTRODUCTION

Generally, mesoporous silica materials, such as those from the MCM and SBA families, have been synthesized by hydrothermal reactions in batch reactors, because they are formed slowly through self-assembly [1-3]. After the discovery of the MCM family of mesoporous materials by Mobil Corporation scientists in 1992 [4,5], the synthesis of surfactant-template mesoporous materials under various conditions has rapidly progressed [6-8]. A new family of mesoporous silica materials with larger pore sizes and thicker pore walls compared to MCM materials, the SBA family, was synthesized at the University of California, Santa Barbara in 1998 [9]. For the synthesis of the SBA family of materials, triblock co-polymer surfactants were used as structure-directing agents (SDAs), and trimethylbenzene (TMB) was used as a swelling agent [3,9-11]. Based on the types of surfactants used and their concentrations, the morphology and structure of the materials can be varied [12-14].

Hydrothermal reactions in batch reactors have drawbacks, such as long reaction times and discontinuous operations [15,16]. In ideal reactions, target materials are produced without any side reactions; however, batch reactors often produce several side products because of their large thermal and concentration gradients [17]. Thus, it is difficult to produce a desired product with high purity. In addition, the amounts of products are also limited to the working capacity of the batch reactor. Continuous flow reactors have several advantages to compensate for the drawbacks of batch reactors [18-20]. Generally, small (including micro-scale) flow reactors offer very short reaction times, rapid heat and mass transfer rates, high-quality homogeneous products, and continuous operations, because the chemical reactions occur in a small confined channel or in droplets formed in the channel [18,21-24]. The quantities of the products are also easily controlled by employing multiple parallel flow reactors [25]. Small channel process devices have been of interest not only for academic investigations but also for applications in many chemical industries [21-25]. Microfluidic systems have also been used to produce nanoparticles of good quality; these systems provide several advantages, such as control of the sizes, morphologies, and size distributions of the nanoparticles [24,26].

Despite the many advantages, there have been only few reports on the successful synthesis of mesoporous silica materials in flow reactors [20,26-28]. This is mainly because of the adverse intrinsic characteristics of flow reactors, such as inhomogeneous flows forming in the channels and channel clogging by solid products [29]. There are two major schemes for flow reactors: continuous and dropwise. In continuous flow reactors [19], different reactants are continuously supplied, mixed, and reacted in series reaction channels. Such reactors have simple construction and are easy to use for many reactions. However, capillary resistance is extremely high because of the pressure-driven flow through the small channels. This leads to inhomogeneity of the products or the clogging of the reaction channels if there are solid products. In dropwise flow reactors [18], uniform droplets in a continuous phase flow through the reaction channels. The drop size is the same size as the diameter of the reaction channel or smaller. Each drop acts as a small batch reactor and the skin friction along the reactor wall can enhance the mixing rate and concentration uniformity of the reactants.

In this work, we used two different arrangements for flow reactions to synthesize a 2D mesoporous silica material, SBA-15: (1) a dropwise flow reaction with active mixing and (2) a dropwise flow reaction using a premixed reactant solution under hydrolysis conditions.

†To whom correspondence should be addressed.
E-mail: hmoon@jnu.ac.kr

## EXPERIMENTAL

### 1. Materials

A block copolymer, $EO_{20}$-$PO_{70}$-$EO_{20}$ (P123), and tetraethylorthosilicate (TEOS) (98%, Sigma-Aldrich) were used as the structure directing agent and silica source, respectively. Hydrochloric acid (37%, Sigma-Aldrich) was used to prepare the acid solutions. Polytetrafluoroethylene (PTFE) tubes were used as reaction channels, and Y junctions were used for the connections. For the dropwise flow reactors, paraffin oil was used as a carrier or continuous phase.

### 2. Synthesis of Mesoporous Silica Materials

The mesoporous silica material, SBA-15, was synthesized by a hydrothermal reaction in a conventional batch reactor [15] to compare with the samples synthesized in the dropwise flow reactors. First, 12.0 g of P123 was dissolved in 480 ml of a 2 M HCl aqueous solution and 90 ml of deionized water. Next, 25.5 g of tetraethyl orthosilicate (TEOS) was added to the solution and stirred for 5 min at room temperature (in this case, the molar ratio of TEOS/P123 was maintained as 60). The mixture was kept in a polypropylene bottle, and the hydrothermal reaction was carried out. The bottle was maintained at 35 °C for 20 h and then 100 °C for 1 day. The product was subsequently filtered and dried at 80 °C for 24 h. The final powder was calcined at 550 °C for 3 h to remove the surfactant P123 and water from the samples.

Later, a dropwise flow reactor for the synthesis of SBA-15 was arranged as shown in Fig. 1. The reactor system consisted of a mixing (or connecting) part and two coiled reaction channels that were immersed in water and oil baths, respectively. Syringe pumps (LSP02-18, Longerpump®) were used to feed the reactant solutions. The channels were constructed from polymer tubes with inner and outer diameters as 1.7 and 2 mm, respectively. Water and oil baths were used to maintain low and high temperatures of 35 and 70-90 °C, respectively. Y junctions were used to combine the two reactant streams and form droplets of the reactant mixture in the oil. The first scheme was a dropwise flow reactor that used only a channel in the high-temperature oil bath. Immiscible inert paraffin oil was used to form reactant drops while it was introduced into the reaction channel through the Y junction. In this scheme, an active mixer with a small magnetic bar was used for mixing the reactant streams prior to droplet formation. This active mixer was used instead of the low-temperature reactor channel operated at 35 °C. The reaction (or retention) time depended on the volume of mixer in the range of 2.5-10 ml. The rotation speed was constantly maintained at 300 rpm. In the second reaction scheme, the two reactant solutions were premixed externally before the drop generator. Every 20 min, the syringe was replaced with a new syringe containing premixed solution to avoid clogging due to premature silica particle formation.

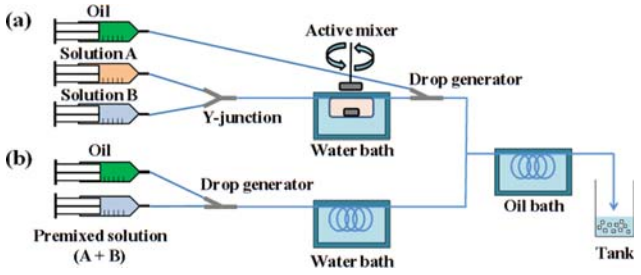


**Fig. 1. Two types of dropwise flow reactors: (a) with active mixing and (b) with premixed solution.**

All the streams for the reaction were prepared using the same recipe for the conventional hydrothermal synthesis of SBA-15 [15]. The final powder products were collected at the end of the hot reaction channel and dried at 80 °C. After the complete removal of water and any trace oil and P123, the samples were calcined at 550 °C for 3 h in air.

### 3. Characterization of Synthesized Materials

X-ray diffraction (XRD) analysis was conducted to identify the crystal structures of all the samples. All XRD patterns were recorded with a high resolution X-ray diffractometer (X'Pert PRO Multi-Purpose X-Ray diffractometer) using a Cu K$\alpha$ radiation source in a $2\theta$ range of 0-10° with a scan speed of 2°/min at 40 kV and 20 mA. The physical properties of all the samples were characterized

**Table 1. Conditions for dropwise flow reaction with active mixing**

| Samples | TEOS (wt%)[a] | P123 (wt%)[a] | Solution pH | Total flow rate[b] (cc/min) | Low temperature reaction sector (active mixer) | | High temperature reaction sector | |
|---|---|---|---|---|---|---|---|---|
| | | | | | Volume[c] (cc) | T (°C) | Length (m) | T (°C) |
| AM1 | 4.20 | 1.98 | <1 | 0.141 | 2.5(60)[d] | 35 | 1.5(25)[d] | 90 |
| AM2 | 4.20 | 1.98 | <1 | 0.141 | 5.0(120)[d] | 35 | 1.5 | 90 |
| AM3 | 4.20 | 1.98 | <1 | 0.141 | 10.0(240)[d] | 35 | 1.5 | 90 |
| AM4 | 4.20 | 1.98 | <1 | 0.141 | 5.0 | 35 | 1.5 | 70 |
| AM5 | 4.20 | 1.98 | <1 | 0.141 | 5.0 | 35 | 1.5 | 80 |
| AM6 | 4.20 | 1.98 | <1 | 0.141 | 5.0 | 35 | 0.75(12.5)[d] | 90 |
| AM7 | 4.20 | 1.98 | <1 | 0.141 | 5.0 | 35 | 3.0(50)[d] | 90 |

[a]wt% of TEOS and P123 in mixed droplets of two reactant solutions (A+B) (TEOS/P123 molar ratio=60)

[b]Ratio of volume flow rates of oil and mixed solution (A+B), $(\frac{\text{oil}}{\text{A+B}})=2$

[c]Volume of active mixer (low temperature reaction)

[d]Residence time in min

by nitrogen adsorption/desorption data measured at 77 K using a BELsorp mini II (SOLETECK). The specific surface areas and mean pore sizes of the samples were evaluated based on Brunauer-Emmett-Teller (BET) and Barrett-Joyner-Halenda (BJH) methods, respectively. The surface morphologies were observed using a JEM-2100F (JEOL) field emission transmission electron microscope (FE-TEM) at 200 kV.

## RESULTS AND DISCUSSION

### 1. Dropwise Flow Reaction with Active Mixing

To overcome the severe clogging encountered in continuous flow reactor systems, a dropwise flow reactor with an active mixer was employed. As shown in Fig. 1(a), the low-temperature reaction channel was replaced with an active mixing chamber with a specified volume, which corresponded to a desired retention (reaction) time. All the operating conditions are listed in Table 1. Based on the recipe used in the conventional batch reaction [15], the concentrations of the two reactants, TEOS and P123, were 4.20 and 1.98 wt%, respectively, corresponding to a TEOS:P123 molar ratio of 60. The total flow rate was 0.141 ml/min, and the volumetric flow rate of paraffin oil was 2 times of that of the mixed reactant solution.

Fig. 2 shows the XRD patterns of the AM series samples synthesized in the dropwise flow reactor with an active mixer. We used three combinations to examine the effects of high reaction temperatures and two reaction times at low and high temperatures after the low reaction temperature was fixed as 35 °C. First, the XRD patterns for samples AM1-AM3 show the results as a function of the reaction time at the low temperature. When the low-temperature reaction time was only 60 min, the three peaks were not clear, which indicates that a low-temperature reaction time of 60 min (the volume of the mixer was 2.5 ml) was not sufficient for the organization into 2D hexagonal structures. When more than 120 min was used, all the XRD peaks were distinct, as shown in Fig. 2. Secondly, the peaks for samples AM2, AM4, and AM5 showed the results in terms of high reaction temperature after the low-temperature reaction for 120 min at 35 °C. When the high reaction temperatures were 70 and 80 °C (AM4 and AM5), one broad peak appeared corresponding to the (100) plane, and the two other peaks corresponding to the (110) and (200) planes were very weak. However, when the high-temperature reaction proceeded at 90 °C, all three peaks (AM2) appeared distinctly. Finally, the three peaks

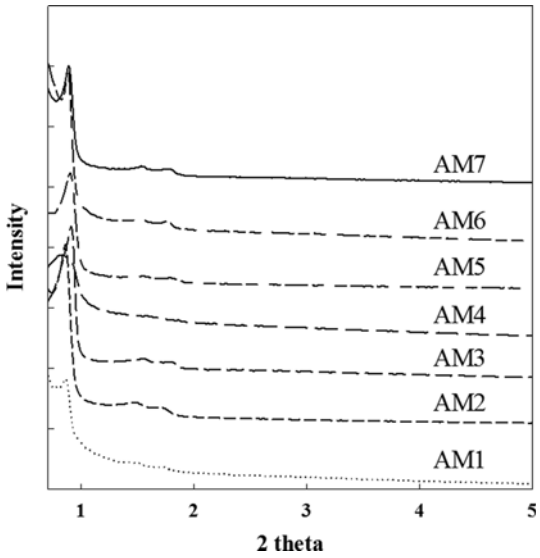


**Fig. 2. X-ray diffraction patterns of AM series samples.**

of AM2, AM6 and AM7 show the XRD results in terms of high temperature reaction time at 90 °C. The first peak corresponding to the (100) plane was not strong when the reaction time was as short as 12.5 min, while XRD spectra for reaction times of more than 25 min showed all three peaks clearly. This indicates that the required high-temperature reaction time is at least 25 min. To prepare a highly ordered mesoporous silica material, namely SBA-15, the reaction time and temperature are important factors. According to the XRD results, 120 min at 35 °C and 25 min with a high temperature over 80 °C are necessary. As listed in Table 2, the d-spacing value for the (100) plane, $d_{100}$, of the AM series samples was in the range of 9.52-10.16 nm, and the wall thickness was as small as 3.54-5.42 nm. The unit cell parameter, a, was calculated from the d-spacing for the (100) peak, $d_{100}$, using the formula $a = 2d_{100}/\sqrt{3}$ and the wall thickness, d, is $a - d_{BJH}$. The XRD characteristics of the AM series samples were comparable with those of SBA-15 reported previously [9,11].

Fig. 3 shows the four typical TEM images from the AM series samples prepared in the dropwise flow reactor. All samples exhibited well-developed hexagonal and mesoporous structure. However, there were many fractured particles. The major reason that fine fractures formed appeared to be the destruction of early-stage embryos of 2D hexagonal silica by the intense mixing in the active

**Table 2. Physicochemical properties of AM series samples**

| Samples | $S_{BET}$ ($m^2/g$) | Total pore volume ($cm^3/g$) | BJH mean pore size (d) (nm) | d-spacing ($d_{100}$) (nm) | Unit cell width (a) (nm) | Wall thickness (w) (nm) |
|---|---|---|---|---|---|---|
| AM1 | 854 | 1.31 | 8.19 | 10.16 | 11.72 | 3.53 |
| AM2 | 927 | 1.29 | 6.30 | 10.14 | 11.72 | 5.42 |
| AM3 | 856 | 0.84 | 7.18 | 9.65 | 11.14 | 3.96 |
| AM4 | 688 | 0.82 | 7.18 | 9.52 | 10.99 | 3.81 |
| AM5 | 829 | 0.78 | 7.18 | 9.64 | 11.13 | 3.95 |
| AM6 | 785 | 1.10 | 7.18 | 9.92 | 11.45 | 4.27 |
| AM7 | 639 | 0.70 | 7.18 | 9.87 | 11.40 | 4.22 |

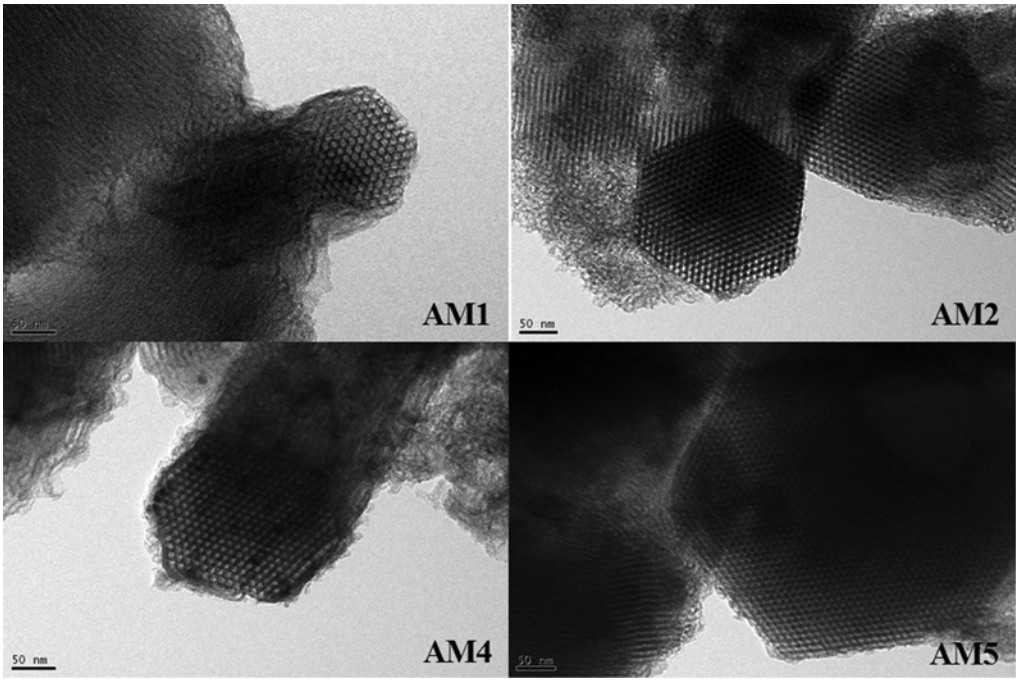


**Fig. 3. TEM results of AM series samples synthesized under different conditions.**

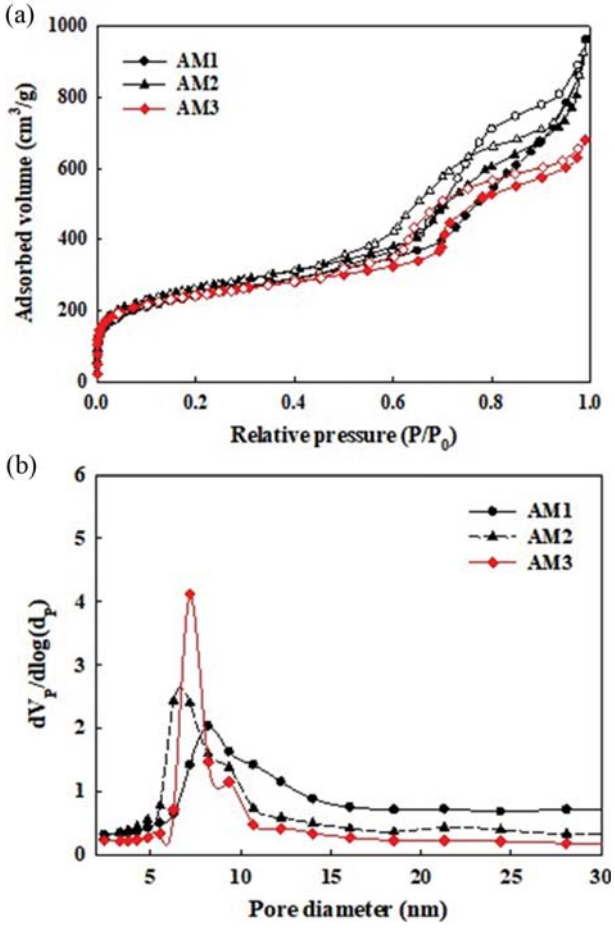


**Fig. 4. Nitrogen isotherms and BJH pore size distributions in terms of reaction time at 35 °C.**

mixer.

Fig. 4 shows the nitrogen adsorption/desorption data measured at 77 K and the BJH pore size distributions of the samples as a function of the reaction time at 35 °C. The nitrogen isotherms were type IV based on the Brunauer-Deming-Deming-Teller (BDDT) classification [12,16]. All the samples showed steep initial increases at low relative pressures, indicating that many small pores had developed. Some research groups previously found that mesoporous silica materials, such as SBA-15, formed micropores due to the penetration of P123 into the walls of 2D hexagonal silica cylinders during their synthesis [30]. The nitrogen isotherms in Fig. 4 show H3 and H4 hysteresis loops with wide ranges at relatively high relative pressures between 0.6-0.9 based on the IUPAC guidelines [31]. They are quite different from H1 loops, which are typically reported for the SBA series [15,32,33]. Typically, the H3 and H4 hysteresis loops represent slit-type mesopores [31], but these were not observed in the TEM images shown in Fig. 3. These unusual hysteresis loops may have arisen from the considerable number of fractured particles and small cavities between them. This result is explained more clearly from the BJH pore size distributions (PSDs) shown in the same figure. None of the samples shown in Fig. 4 possessed uniform PSDs, indicating that a wide distribution of large pores formed in or between the agglomerates of the fractured particles, as mentioned above. When the reaction time was 60 min at 35 °C, the BJH pore size distribution was very broad, but the peak of PSD became sharper as the low-temperature reaction time increased. This indicates that a sufficient reaction time at a low temperature is quite important for the synthesis of SBA-15 in dropwise flow reactor systems.

In the high-temperature reaction channel, the reaction temperature and time are also important factors. Figs. 5 and 6 show the

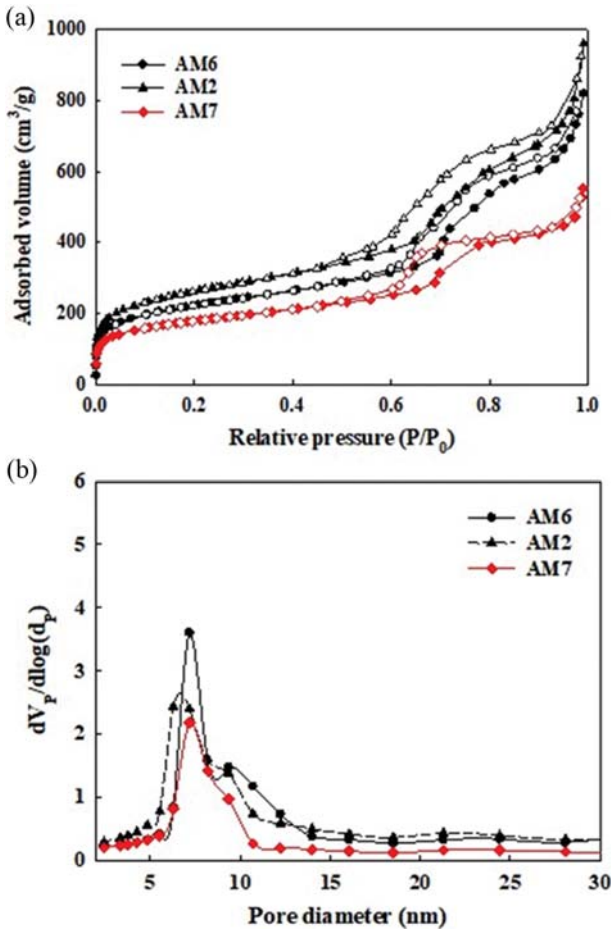


**Fig. 5. Nitrogen isotherms and BJH pore size distributions in terms of reaction time at 90 °C.**

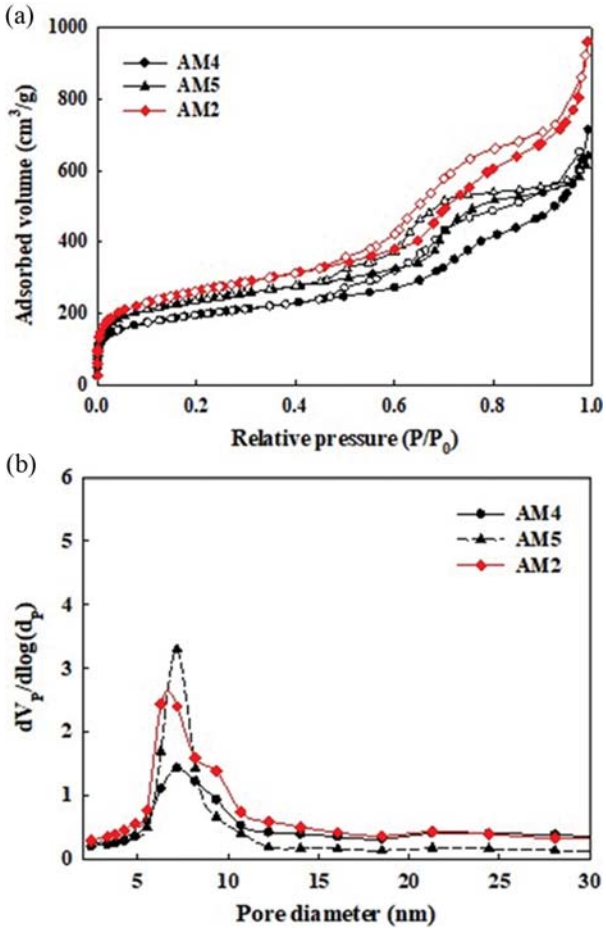


**Fig. 6. Nitrogen isotherms and BJH pore size distributions in terms of high reaction temperature.**

nitrogen adsorption isotherms and BJH pore size distributions of the other AM series samples, obtained under different conditions. Fig. 5 shows the effect of the reaction time at a high reaction temperature of 90 °C. For reaction times of 12.5, 25, and 50 min, there were no changes in the BET surface area, total pore volume, and mean BJH pore size of the samples; however, the pore size distribution became more uniform with increasing reaction time. The effect of the high reaction temperature is shown in Fig. 6. As the reaction temperature was increased from 70 to 90 °C, the hysteresis became steeper, approaching an H1-type loop, and the PSDs become uniform (in particular, the PSD of the sample AM5 obtained at 80 °C looks better). This indicates that after forming a 2D hexagonal structure at low temperature, the structure can become stronger or more durable due to the regular stacking that occurs during the high-temperature reaction. For all the AM series samples, as shown in Table 2, the BET surface area, total pore volume, and BJH mean pore size were in the ranges of 639-927 $m^2/g$, 0.70-1.39 cc/g, and 6.30-8.10 nm, respectively, which are comparable to the corresponding values of SBA-15 reported in many previous works [9, 11,15].

**2. Dropwise Flow Reaction Using Premixed Reactant Solution**

To prevent the formation of fractured products, a second synthesis method for SBA-15 was used in which the two reactants were premixed prior to the low-temperature reaction channel, as shown in Fig. 1(b). In this scheme, various amounts of TEOS and P123 (the same as for the AM series samples) were mixed for about 5 min in a 2 M hydrochloric solution and directly fed into the low-temperature reaction channel maintained at 35 °C through a drop generator. According to the results in the previous section (for AM5), the reaction times used at the low temperature (35 °C) and high temperature (80 °C) were fixed at 120 and 25 min, respectively.

Fig. 7 shows the XRD and TEM results of sample SBA-15F, which was synthesized using the premixed reactant solution in the dropwise flow reactor, as well as those of the reference sample SBA-15B, which was synthesized in a conventional batch reactor with the same recipe. Based on the XRD results, the two samples produced three typical peaks corresponding to the (100), (110), and (200) planes, representing 2D hexagonal structures. As listed in Table 3, the d-spacing values, $d_{100}$, were (9.16, 9.27) and the unit cell parameters were (10.58, 10.70) for SBA-15B and SBA-15F, respectively. The TEM results also showed clear 2D hexagonal structures of mesoporous silica; the grain size of SBA-15B was larger than that of SBA-15F. SBA-15F still contained fractured particles, indicating that the wall shear stress could break the solid products when they were flowing through the reaction channel.

Fig. 8 shows the nitrogen adsorption/desorption isotherms and

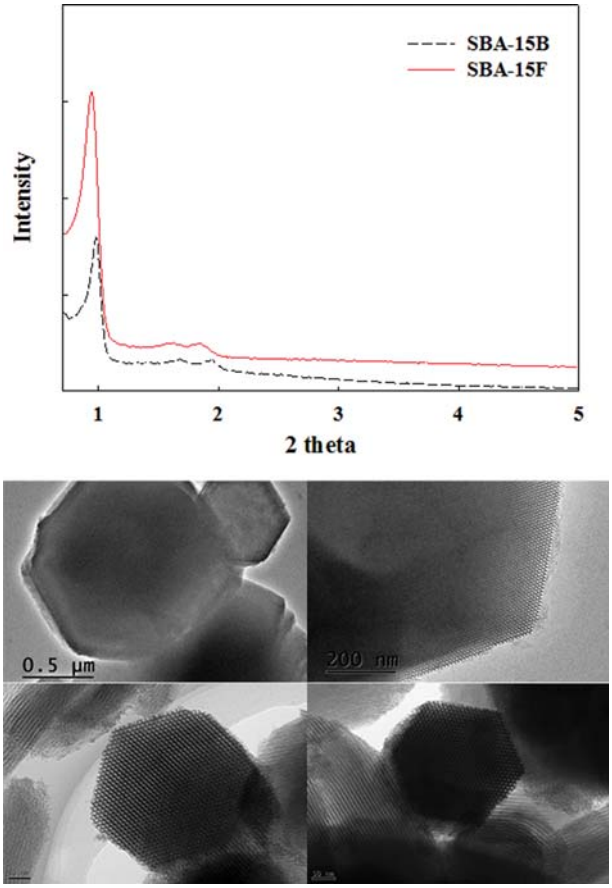


**Fig. 7. XRD patterns and TEM images of SBA-15B (above) and SBA-15F (below).**

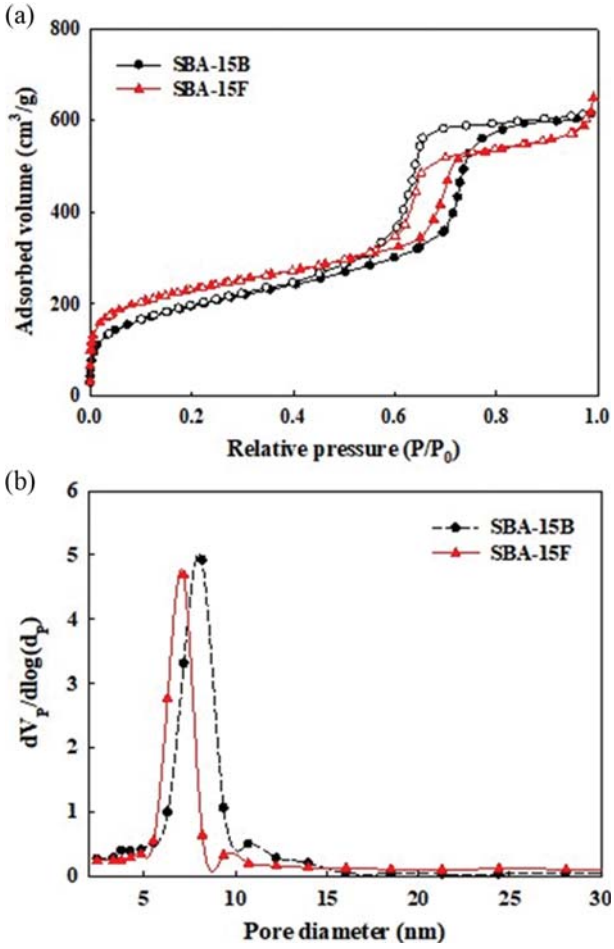


**Fig. 8. Nitrogen isotherms and BJH pore size distributions of SBA-15B and SBA-15F.**

BJH PSDs of the two samples. Although they had similar unit cell parameters, the mesopore fractions and PSDs were considerably different. The BJH mean pore sizes of SBA-15B and SBA-15F, as shown in Table 3, were 8.19 and 7.18 nm, respectively. Accordingly, the wall thickness was 2.39 and 3.52 nm, respectively, indicating that SBA-15F had thicker pore walls than SBA-15B, but agreed well with previously reported results [15]. In addition, Fig. 8 shows that the two samples had similar PSDs with different mean pore sizes. The BET surface area and total pore volume of SBA-15F were 818 $m^2/g$ and 0.82 cc/g, respectively, which are comparable with those for SBA-15B.

## CONCLUSIONS

The samples produced using a dropwise flow reactor with an active mixer (as a low-temperature reaction sector) exhibited good XRD patterns for (100), (110), and (200) planes. However, their nitrogen isotherms showed unexpected hysteresis loops (H3 or H4 types) and wide pore size distributions. These results were due to the widely distributed small pores that developed in and between the agglomerates of fractured particles. However, when samples were synthesized with a premixed solution, most of the characterization results matched well with the corresponding values of the reference SBA-15, which was synthesized with the same recipe in a conventional batch reactor.

Based on the formation of fractured particles in the product, mixing and wall effects are important in flow reactors, even in the dropwise flow reactor system. Once reliable techniques to prevent

**Table 3. Comparison of SBA-15B and SBA-15F**

| Samples | $S_{BET}$ ($m^2/g$) | Total pore volume ($cm^3/g$) | BJH mean pore size (d) (nm) | d-spacing ($d_{100}$) (nm) | Unit cell width (a) (nm) | Wall thickness (w) (nm) |
|---|---|---|---|---|---|---|
| SBA-15B[a] | 700 | 0.86 | 8.19 | 9.16 | 10.58 | 2.39 |
| SBA-15F[b] | 818 | 0.82 | 7.18 | 9.27 | 10.70 | 3.52 |

[a]Synthesized by conventional batch reaction
[b]Synthesized in the dropwise flow reactor using premixed solution

the clogging of reaction channels and the formation of fractures are devised, this dropwise flow reactor system should be a plausible process to prepare highly ordered and homogeneous 2D hexagonal mesoporous silica materials quickly and continuously. Ultimately, the manufactured SBA-15 could be widely used for many applications such as sensors, adsorption, catalysis, ion exchange and drug delivery systems [34].

## ACKNOWLEDGEMENTS

This research was supported by the National Research Foundation, Republic of Korea (NRF-2017R1A1B03032488).

## REFERENCES

1. J. M. Kim and R. Ryoo, *Chem. Commun*., 259 (1998).
2. A. Sayari, B. H. Han and Y. Yang, *J. Am. Chem. Soc*., **126**, 14348 (2004).
3. T. P. B. Nguyen, J. W. Lee, W. G. Shim and H. Moon, *Micropor. Mesopor. Mater*., **110**, 560 (2008).
4. C. T. Kresge, M. E. Leonowicz, W. J. Roth, J. C. Vartuli and J. S. Beck, *Nature*, **359**, 710 (1992).
5. J. S. Beck, J. C. Vartuli, W. J. Roth, M. E. Leonowicz, C. T. Kresge, K. D. Schmitt, C. T. W. Chu, D. H. Olson, E. W. Sheppard, S. B. McCullen, J. B. Higgins and J. L. Schlenker, *J. Am. Chem. Soc*., **114**, 10834 (1992).
6. K. Schumacher, M. Grün and K. K. Unger, *Micropor. Mesopor. Mater*., **27**, 201 (1999).
7. D. Kumar, K. Schumacher, C. du Fresne von Hohenesche, M. Grün and K. K. Unger, *Colloids Surf., A*, **109**, 187 (2001).
8. L. Wang, J. Zhang and F. Chen, *Micropor. Mesopor. Mater*., **122**, 229 (2009).
9. D. Zhao, J. Feng, Q. Huo, N. Melosh, G. H. Fredrickson, B. F. Chmelka and G. D. Stucky, *Science*, **279**, 548 (1998).
10. D. Zhao, Q. Huo, J. Feng, B. F. Chmelka and G. D. Stucky, *J. Am. Chem. Soc*., **120**, 6024 (1998).
11. A. Katiyar, S. Yadav, P. G. Smirniotis and N. G. Pinto, *J. Chromatogr. A*, **1122**, 13 (2006).
12. D. Zhao, J. Sun, Q. Li and G. D. Stucky, *Chem. Mater*., **12**, 275 (2000).
13. N. Zucchetto, M. J. Reber, L. Pestalozzi, R. Schmid, A. Neels and D. Brühwiler, *Micropor. Mesopor. Mater*., **257**, 232 (2018).
14. K. Kosuge, T. Sato, N. Kikukawa and M. Takemori, *Chem. Mater*., **16**, 899 (2004).
15. S. C. Ryu, J. Y. Kim, M. J. Hwang and H. Moon, *Korean J. Chem. Eng*., **35**, 489 (2018).
16. J. W. Lee, D. L. Cho, W. G. Shim and H. Moon, *Korean J. Chem. Eng*., **21**, 246 (2004).
17. S. K. W. Dertinger, D. T. Chiu, N. L. Jeon and G. M. Whitesides, *Anal. Chem*., **73**, 1240 (2001).
18. M. Faustini, J. Kim, G.-Y. Jeong, J. Y. Kim, H. R. Moon, W. S. Ahn and D. P. Kim, *J. Am. Chem. Soc*., **135**, 14619 (2013).
19. L. Xu, C. Srinivasakannan, J. Peng, D. Zhang and G. Chen, *Chem. Eng. Process*., **93**, 44 (2015).
20. T. N. Ng, X. Q. Chen and K. L. Yeung, *RSC Adv*., **5**, 13331 (2015).
21. H. Pennemann, P. Watts, S. J. Haswell, V. Hessel and H. Löwe, *Org. Process Res. Dev*., **8**, 422 (2004).
22. G. M. Whitesides, *Nature*, **442**, 368 (2006).
23. N. Kockmann and D. M. Roberge, *Chem. Eng. Process*., **50**, 1017 (2011).
24. J. Wagner and J. M. Köhler, *Nano Lett*., **5**, 685 (2005).
25. A. Yavorskyy, O. Shvydkiv, N. Hoffmann, K. Nolan and M. Oelgemoller, *Org. Lett*., **14**, 4342 (2012).
26. T. Vandermeersch, T. R. C. Van Assche, J. F. M. Denayer and W. De Malsche, *Micropor. Mesopor. Mater*., **226**, 133 (2016).
27. N. Hao, Y. Nie and J. X. J. Zhang, *ACS Sustainable Chem. Eng*., **6**, 1522 (2018).
28. C. L. Tong, R. A. Boulos, C. Yu, K. S. Iyer and C. L. Raston, *RSC Adv*., **3**, 18767 (2013).
29. S. L. Poe, M. A. Cummings, M. P. Haaf and D. T. McQuade, *Angew. Chem. Int. Ed*., **45**, 1544 (2006).
30. M. Choi, W. Heo, F. Kleitz and R. Ryo, *Chem. Commun*., 1340 (2003).
31. W. Wang, P. Liu, M. Zhang, J. Hu and F. Xing, *Open J. Compos. Mater*., **2**, 104 (2012).
32. N. Hiyoshi, K. Yogo and T. Yashima, *Micropor. Mesopor. Mater*., **84**, 357 (2005).
33. J. Aguado, J. M. Arsuaga, A. Arencibia, M. Lindo and V. Gascón, *J. Hazard. Mater*., **163**, 213 (2009).
34. Z. S. Ern, S. Tuncer, G. Gezer, L. T. Yildirim, S. Banerjee and A. Yilmaz, *Micropor. Mesopor. Mater*., **235**, 211 (2016).